Journal of the European Ceramic Society 21 (2001) 2353–2360

www.elsevier.com/locate/jeurceramsoc

$MoSi_2/Al_2O_3$ FGM: elaboration by tape casting and SHS

Anne-Laure Dumont [a,b], Jean-Pierre Bonnet [b], Thierry Chartier [c,*], José M.F. Ferreira [a]

[a] *Department of Ceramics and Glass Engineering, UIMC, 3810-193 Aveiro, Portugal*
[b] *GEMH-ENSCI, 87065 Limoges Cedex, France*
[c] *Laboratoire de Science des Procedes, Ceramiques et de Traitements de Surface, UMR 6638, CNRS-ENSCI, 47–73 Av. Albert Thomas, 87065 Limoges Cedex, France*

Received 19 October 2000; received in revised form 5 January 2001; accepted 12 January 2001

Abstract

$MoSi_2/Al_2O_3$ functionally graded materials (FGM) with alumina contents varying from 20 to 80 mol% have been fabricated using a combination of tape casting and self-propagating high-temperature synthesis (SHS). Tape casting was used to prepare tapes of different compositions. Square units cut out of tapes with different compositions were stacked in a variety of sequences. After debinding, the green samples were ignited at room temperature. The combustion reactions were conducted under a weak load to enhance the densification of the composition-graded composites. The variation of porosity as a function of the applied pressure and of the thickness of the layers was investigated. The electrical resistivity of the as-obtained FGM varies by more than 10 orders of magnitude across the composite. © 2001 Published by Elsevier Science Ltd.

Keywords: Electrical properties; FGM; $MoSi_2/Al_2O_3$; Composites; SHS; Tape-casting

1. Introduction

The intermetallic $MoSi_2$ has been extensively studied during the past 20 years for its rather low density (6.31 g/cm^3), high electrical conductivity and very good oxidation resistance at high temperature, even in very aggressive environments.[1–11] The main limitation for its widespread application at high temperature comes from a brittle-to-ductile transition at 900–1000°C that confers $MoSi_2$ with a very low creep resistance at a temperature higher than 1200°C.[12,13] Alumina is an oxide known for its low density (3.98 g/cm^3), high electrical resistivity and excellent creep resistance even at temperatures higher than 1400°C.[14,15] The coefficients of thermal expansion (CTE) of $MoSi_2$ and Al_2O_3 are very similar between 20 and 1400°C. Dense $MoSi_2/Al_2O_3$ composites have already been fabricated by sintering [2] or by SHS.[4,16–20] Multilayer $MoSi_2/Al_2O_3$ composites with alternate conducting and insulating layers [21] were also prepared via the SHS process.

The preparation of $MoSi_2/Al_2O_3$ multilayer functionnally graded materials (FGM) with alumina contents progressively varying through the sample from 20 to 80 mol% is the aim of the present work. This has a potential application in electrical devices combining the high electrical conductivity of $MoSi_2$ (see Table 1) and the high mechanical properties of Al_2O_3. In this context $MoSi_2/Al_2O_3$ FGM were prepared by combining tape casting and SHS and the gradient of the electrical properties was determined.

2. Composition of reactive mixtures

The combustion systems used are mixtures of solid compounds. The two most exothermic reactions leading to the synthesis of both alumina and molybdenum disilicide are the following:

$$MoO_3 + 2Si + 2Al \rightarrow MoSi_2 + Al_2O_3 \quad (1)$$

$$MoO_3 + 2SiO_2 + 14/3Al \rightarrow MoOSi_2 + 7/3Al_2O_3 \quad (2)$$

The variation of standard enthalpy of these two reactions at 25°C are given in Table 2,[22] as well as their

* Corresponding author. Tel.: +33-5-55-452222; fax: +33-5-55-790998.
E-mail address: t.chartier@ensci.fr (T. Chartier).

0955-2219/01/$ - see front matter © 2001 Published by Elsevier Science Ltd.
PII: S0955-2219(01)00198-4

Table 1
Some characteristics of $MoSi_2$ and Al_2O_3 materials[12,13]

Material	$MoSi_2$	Al_2O_3
C.T.E ($°C^{-1}$) (20–1400°C)	$\approx 8.10^{-6}$–14.10^{-6}	$\approx 8.10^{-6}$–14.10^{-6}
Young's modulus (GPa) at 25°C	≈440	≈400
Melting temperature (°C)	2020	2054
Electrical behaviour	Conductor	Insulator
Creep resistance	Low for $T > 900$°C	High, even for $T > 1400$°C

Table 2
Variation of standard enthalpy of reaction ($\Delta_R H°$) at 25°C and value of adiabatic temperature for an ignition at 25°C

Reaction	$\Delta_R H°$ (J/mol)	T(ad) (°C)
(1)	−1 062 326	3285
(2)	−1 475 193	2575

adiabatic temperatures calculated for the ignition of the stoichiometric compositions at 25°C.

As the adiabatic temperatures of both reactions are far above the melting temperature of the products of reaction, the mixtures are assumed to completely melt during the combustion synthesis. Previous studies[17,18] have shown that during this complete melting of products, two immiscible liquid phases form and separate, yielding to a very rough microstructure. This microstructure can be described as a heterogeneous distribution of large (10 μm to 2 mm) silicide-based domains ($Mo(Si,Al)_2$ and Mo_5Si_3) in an alumino-silicate matrix (Al_2O_3 grains surrounded by an intergranular phase containing Al, Si and O). A homogeneous distribution of small inclusions of the minor phase in the matrix [17–19] can be obtained when products only partially melt during the SHS reaction. The control of the amount of liquid formed during the process is possible only if the maximum temperature reached during reactions is the melting temperature of the products of reaction. This control can easily be achieved by diluting the systems, i.e. by adding inert powders (here final products Al_2O_3 and/or $MoSi_2$) to the reactant mixtures, in such a way that the heat released by reactions (1) or (2) (unchanged) is dissipated in a larger amount of product. The chemical composition of the constituents of a homogeneous composite are summarised in Table 3.[17]

A previous study,[21] dealing with the fabrication of multilayer $MoSi_2/Al_2O_3$ composites with alternate conducting and insulating layers, has also shown the major influence of the amount of liquid formed in each layer during the SHS reaction on the maintenance of a laminar structure in the final component. The multilayer structure was conserved only for amounts of liquid less than 35 vol.%. Hence, in the systems considered here, appropriate amounts of each of the final products (i.e. $MoSi_2$ and Al_2O_3) have been added to the reactants in order to accurately control both the amount of transient liquid formed and the final $Al_2O_3/MoSi_2$ molar ratio in each layer. The compositions of the final powder mixtures used in this study, the theoretical final amounts of $MoSi_2$ in the corresponding layers and the theoretical quantities of liquid formed during the SHS reaction are indicated in Table 4.

3. Preparation of the FGM

3.1. Flow chart

The $MoSi_2/Al_2O_3$ composite based functionally-graded materials (FGM) were made by stacking reactive layers of different compositions previously prepared by tape-casting. The three types of stacking studied are shown in Fig. 1. They correspond to a composite with a continuous increase of Al_2O_3 concentration from one side to the other (a-type), to symmetrical gradients with Al_2O_3-rich external layers (b-type), or with $MoSi_2$-rich external layers (c-type).

The flow chart of the process used to prepare the FGM components is presented in Fig. 2.

3.2. Preparation of the layers

The characteristics of the commercial powders used to prepare the seven reactive mixtures (Table 4) are presented in Table 5.

Table 3
Results of chemical (energy dispersive X-rays EDX) and X-ray diffraction analyses obtained on $MoSi_2/Al_2O_3$ composites after a partial melting of the products during the SHS reaction[17]

Constituents of the liquid formed during SHS reaction	Crystallised phases observed after cooling (X-ray diffraction)	Chemical composition of grains (EDX analysis)
Al, O, Si	Al_2O_3, mullite (traces)	
Mo, Si, traces of Al	$MoSi_2$, Mo_5Si_3, sometimes traces of $Mo(Si,Al)_2$	$Mo_{0.36}Si_{0.64}$ ($MoSi_2$)

Table 4
The different amounts of each reactant and diluant introduced in each layer composition, and the theoretical amounts of liquid formed during the SHS reaction

Final composition of the layer ($MoSi_2$ mol%)	20	30	40	50	60	70	80	
Mass of each reactant and diluant to prepare 100 g of reactive mixture	MoO_3 (g)	23.583	30.755	21.890	19.315	17.676	23.461	20.261
	Si (g)	0	12.002	0	0	0	9.156	7.907
	SiO_2 (g)	19.688	0	18.275	16.125	14.757	0	0
	Al (g)	20.630	11.530	19.149	16.896	15.462	8.796	7.596
	$MoSi_2$ (g)	2.243	6.500	26.731	39.455	50.435	52.889	64.236
	Al_2O_3 (g)	33.856	39.213	13.955	8.209	1.669	5.698	0
Theoretical vol.% of liquid formed during SHS reaction	19	29	31	24	23	24	18	
Type of reaction	(2)	(1)	(2)	(2)	(2)	(1)	(1)	
Vol.% $MoSi_2$	18.99	28.66	38.46	48.39	58.44	68.63	78.95	

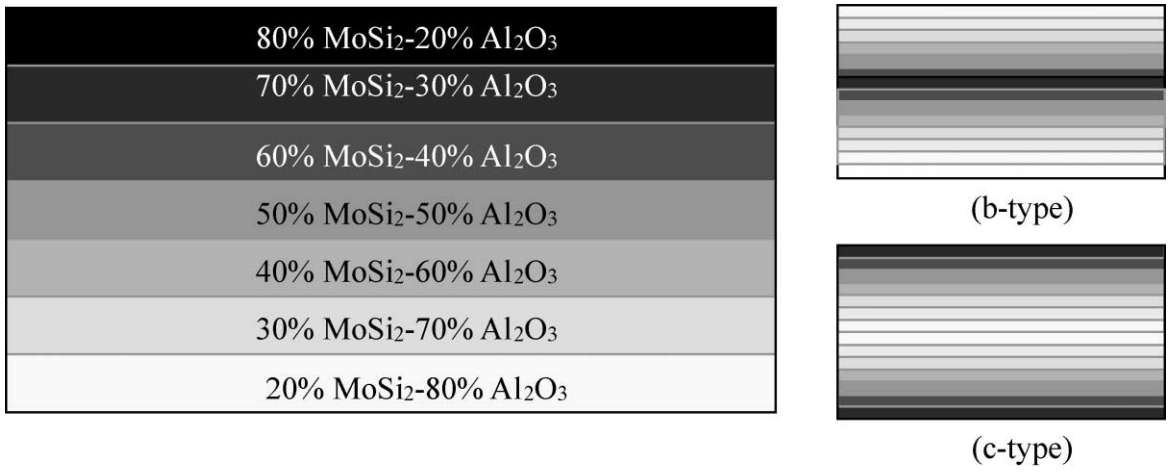

Fig. 1. Schematic representation of the different kinds of FGM prepared.

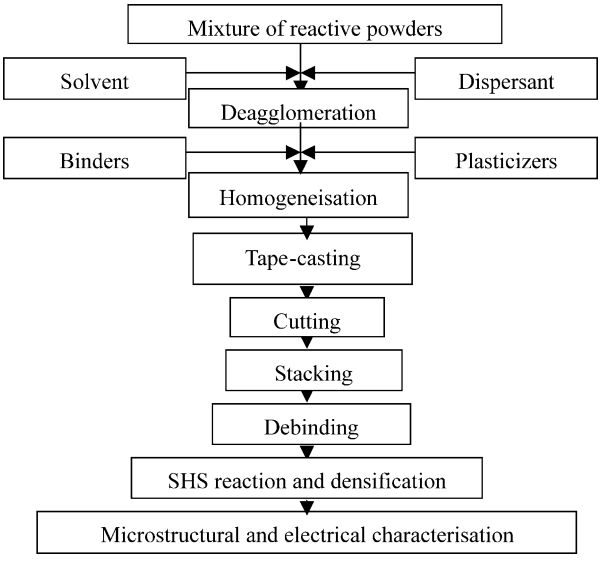

Fig. 2. Flow chart of the fabrication of the FGM components.

Organic additives were added to the powders in order to obtain slurries with a viscosity and a rheological behaviour suitable for tape casting. The solvent was an azeotropic mixture containing 66 vol.% methyl-ethyl-keton (MEK) and 34 vol.% ethanol. The dispersant was a phosphate ester. The binder was a polyvinyl-butyral (PVB) and the plasticizer was dibutylphtalate (DBP).[23] The composition of a slurry is given in Table 6.

The preparation of the slurries was performed in two stages. The first one was the deagglomeration and the dispersion of the powders, by ball-milling during 2 h in the dispersant-solvent-powder system. Then, the binder and the plasticizer were added and the slurry was homogenised by ball milling for 12 h. The viscosity was adjusted by adding solvent.

Tape casting was performed using the "doctor-blade method" on a polypropylene film. Two opening gaps between the moving blade and the support were fixed at 500 and 800 μm leading to shear rates of 10 and 6.25 s^{-1}, respectively, for a casting speed of 5.10^{-3} m/s. The

Table 5
Characteristics of the commercial powders used

	Nature	Supplier	Mean particle size (μm)
Reactants	MoO_3	Aldrich, 99.5% purity	$d_{50}=9.78$
	Si	Aldrich, 99% purity	$d_{50}=10.97$
	SiO_2	P600, Sifraco France	$d_{50}=4$
	Al	AlliedSignal	$d_{50}=80$
Additives for dilution	$MoSi_2$	Aldrich, 99% purity	$d_{50}=2.78$
	Al_2O_3	Alcoa	$d_{50}=1$

Table 6
Mass of the different organics added to 100 g of reactive powder during the preparation of the slurries

Reactive mixture	MEK–EtOH	Phosphate ester	PVB (g)	DBP (g)
100 g	27.3–36 g	1 g	3.5 g	5.6 g

drying of the tapes was performed at room temperature in static air for 24 h.

3.3. Green stacking realisation

The dried tapes were cut into 3.5×3.5 cm^2 square units and removed from their polypropylene support. The thickness of the dried tapes ranged from 210 to 280 μm and from 350 to 450 μm for the 500 and 800 μm gaps, respectively. Squares of the different compositions were stacked in appropriate order and the green stackings were pressed at room temperature under a pressure of 0.3 MPa. Their debinding was performed under flowing air at a maximum temperature of 320°C.

3.4. Reaction and densification of FGM

The green components were put in a crucible composed of two parts: a metallic part to ensure mechanical resistance and a refractory part to provide thermal resistance (Fig. 3). The reactor worked in air under atmospheric pressure. A piston applied a constant pressure on the sample. A given mass placed above the piston allowed the application of a constant pressure, irrespective of the degree of shrinkage of the sample during densification. A U-shaped Kanthal wire connected to an electrical power supply was placed inside the crucible, close to one vertical side of the pellet. The part of the wire in contact with the reactive sample was covered by a small amount of powder mixture corresponding to the stoichiometry of reaction (1).

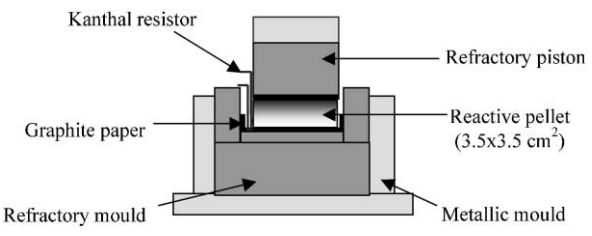

Fig. 3. Schematic of the reactor used for combustion synthesis of FGM.

The reaction was ignited by applying a current to the Kanthal resistor for a few seconds. The heat released ignited the exothermic reaction in the reactive powder located around the wire and the reaction then propagated from the upper face to the bottom of the pellet, throughout the sample, in a few seconds. After propagation, the natural cooling of the component was very fast (from 2000 to 600°C in about 30 s).

4. Influence of the applied pressure on the multilayer structure of the FGM

Some combustion trials were carried out without any applied pressure. A delamination of the different layers was observed on the pellets (Fig. 4a).

The application of a low pressure, between 0.9 and 3.4 MPa, significantly increased the adherence between the layers and the density of the FGM (Fig. 4). When a 1.4 MPa pressure was applied before the ignition and maintained during the SHS reaction and the cooling period, the adherence between the different layers became satisfactory but a large amount of porosity still remained, particularly in the centre of the component (Fig. 4b). The porosity decreased significantly when the applied pressure increased (Fig. 4c). The largest pores completely disappeared when the applied pressure was 3.4 MPa.

Whatever the value of the applied pressure, the microstructure of samples was regular and each layer presented a homogeneous distribution of the minor phase inside the matrix (Fig. 5). A Mo_5Si_3 phase can be observed in an intergranular position around the $MoSi_2$ grains (lightest areas Fig. 5a).

5. Characterisation of the FGM components

5.1. Microstructure

Backscattered SEM micrographs have been taken for the cross-section of samples made of thin or thick layers. Image analysis was performed in order to evaluate the gradient of Al_2O_3, $MoSi_2$ and porosity contents from side to side of the sample. Results obtained for an a-type FGM component prepared from thick layers (350–450 μm) are reported in Fig. 6. The Al_2O_3 and $MoSi_2$ contents which are shown correspond to the sample skeleton. The variation of the content of both solids across the FGM component corresponds to the original aim, i.e. a succession of individually homogeneous compositions

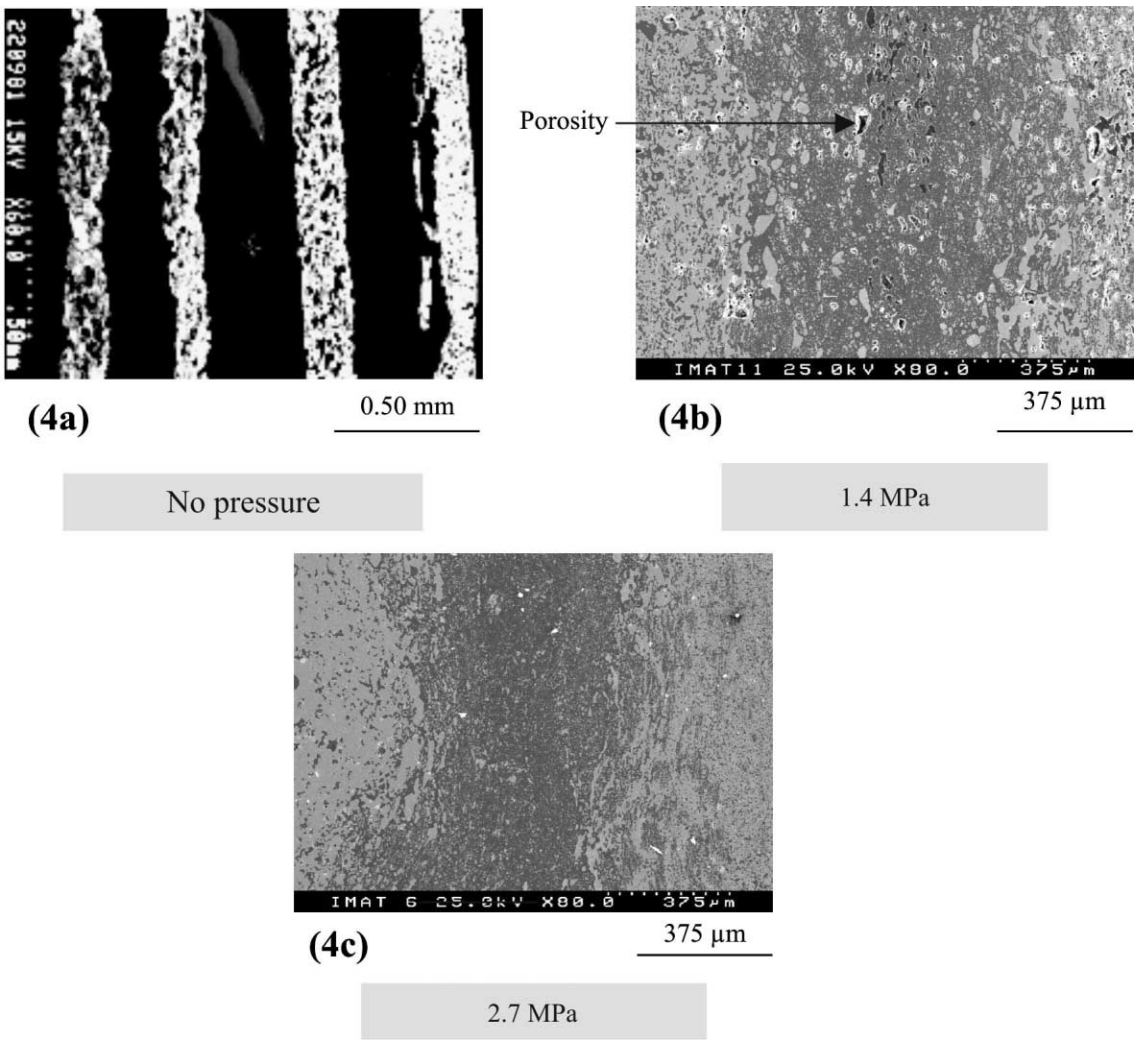

Fig. 4. Microstructure of different samples. (a) FGM reacted under no pressure (back scattering electrons); (b) FGM reacted under 1.4 MPa (c-type FGM, secondary electrons); (c) FGM reacted under 2.7 MPa (c-type FGM, secondary electrons).

varying approximately from 21 to 81 vol.% Al_2O_3 and from 79 to 19 vol.% $MoSi_2$. The multilayer structure has been conserved during the SHS reaction. A decrease in the thickness of the component layers leads to a porosity increase. The porosity in the middle of the component increases from 0.5 to 10% when the thickness of the dried tapes decreases from 400 to 250 µm. The presence of interfaces, which slow down the propagation rate of the reaction, promotes heat losses by conduction, convection and radiation. Therefore, the use of thin layers leads to a decrease of the energy available for heating the sample. For the same composition, the amount of liquid formed during the SHS stage is lower in the thin layers compared to thick layers and the effect of the applied pressure is thus less efficient.

5.2. Electrical resistivity

A two point method was used to measure the room-temperature resistivity of the sample in a direction perpendicular to the layers. After the first measurement, the surface containing the highest alumina content was polished and a thickness of about 50 µm was removed. New electrodes were deposited and the resistivity of the polished FGM was measured. This operation was reiterated until the FGM became too thin. The results obtained for an a-type component are shown in Fig. 7. The upper surface of the component corresponded to the highest alumina content. The electrical resistivity of the starting FGM (before any polishing) is very high (about 150 MΩ.cm). When the 20% $MoSi_2$ layer is removed, the electrical resistivity falls to about 150 Ω.cm. After elimination of the 20, 30 and 40% $MoSi_2$ layer, the electrical resistivity falls to about 0.3 Ω cm and remains constant for further thickness which is removed.

For comparison, samples of each composition constituting the layers were synthesised under a pressure of 3.4 MPa and their room-temperature electrical resistivity was measured using the 2 point method. The room temperature resistivities measured for mono-composition

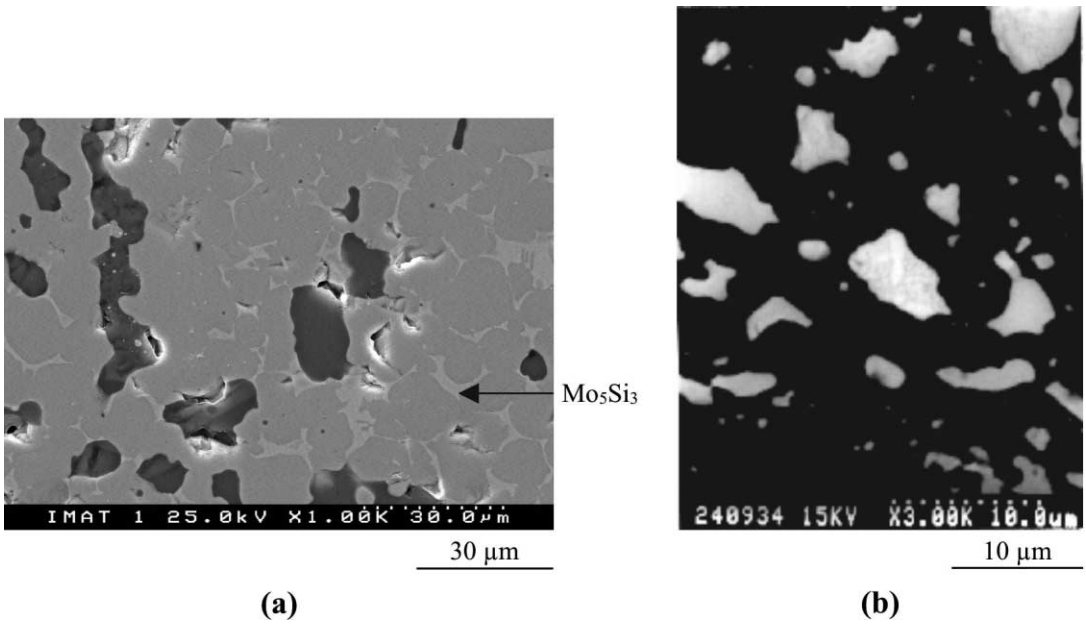

Fig. 5. Backscattered electron micrographs showing microstructure of (a) $MoSi_2$-rich layer containing alumina inclusions (applied pressure 2.4 MPa); (b) Al_2O_3-rich layer containing $MoSi_2$ inclusions (applied pressure 0.9 MPa).

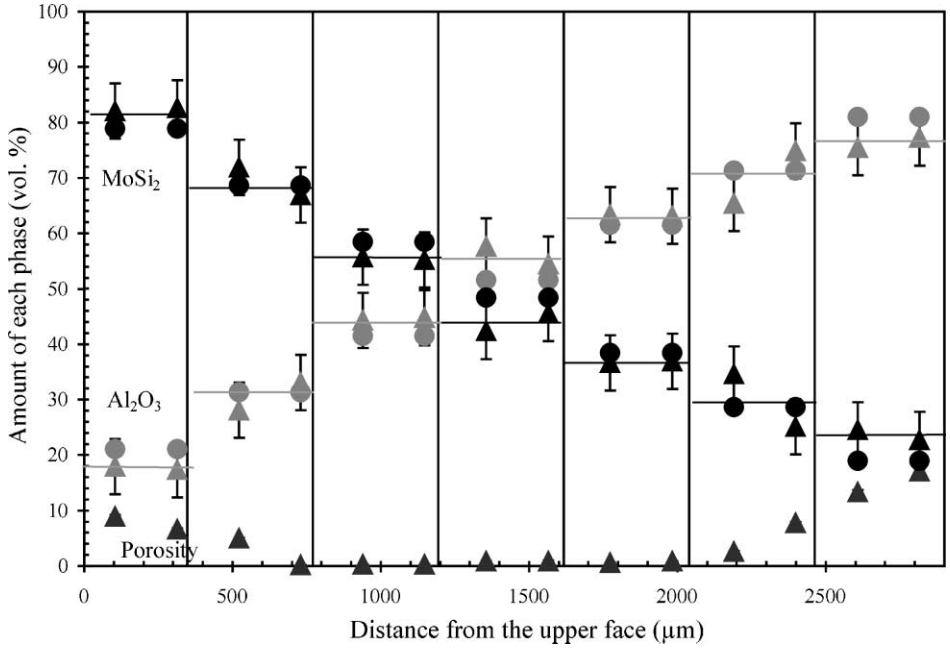

Fig. 6. Variation of the amount (vol.%) of Al_2O_3, $MoSi_2$ and porosity across an a-type FGM component. The reactive pellet was made by stacking layers of the 7 different compositions; each component layer was composed of three identical green thick layers. The sample has been densified under 3.4 MPa. The circular points represent the Al_2O_3 and $MoSi_2$ contents calculated from the starting tape composition. The triangular points are the experimental values. Lines correspond to the mean value of experimental points.

samples with the same composition as the layer in contact with electrodes are also indicated in Fig. 7. The resistivity of each layer of the multilayer component is mainly controlled by the average composition of the layer. The interactions between layers, which occur during the SHS stage, have a very weak influence on the evolution of the resistivity across the FGM component. However, the electrical behaviour in the interface proximity is modified. The affected zone is thicker for the more resistive layers. The introduction of small amounts of $MoSi_2$ in the resistive layer favours percolation between conductive particles, especially if these are located at grain boundaries.

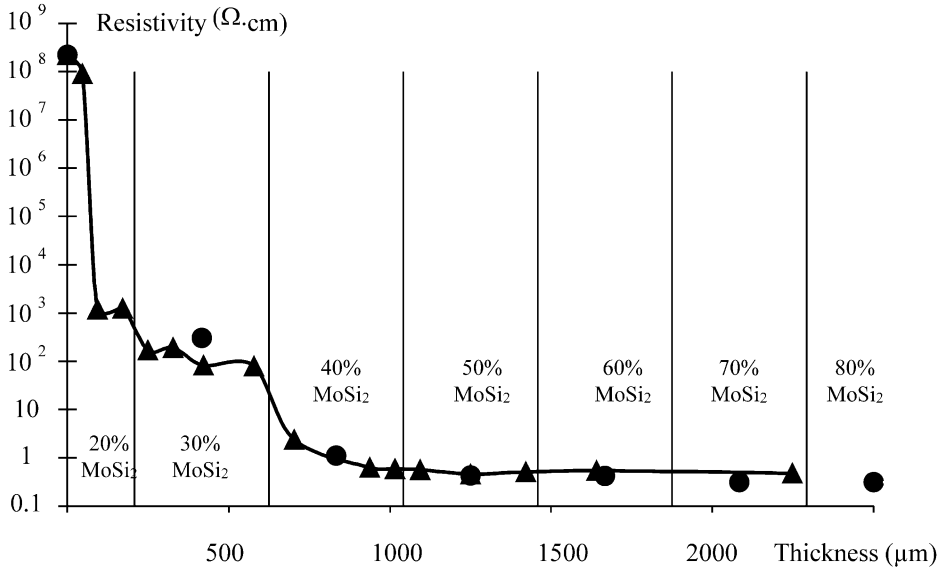

Fig. 7. Evolution of resistivity across an a-type FGM (▲) and resistivity of mono-composition samples (●) with the average layer composition.

6. Conclusion

The association of tape-casting and SHS has been used to prepare $MoSi_2/Al_2O_3$ based FGM components with various kinds of composition gradients. A strong room-temperature resistivity gradient (from 1.5×10^8 to 0.3 Ω cm) is observed in the domain where the amount of $MoSi_2$ changes from 20 to 40-vol.%. The porosity of the multilayer samples is significantly reduced when a low pressure (typically 3 MPa) is applied during the SHS stage and when the green layer thickness is greater than 500 μm. The conservation of the multilayer structure is strongly dependent on the control of the amount of liquid formed during the SHS reaction. When the theoretical amount of liquid in each layer is less than 35 vol.%, a FGM component can be obtained with an alumina content varying across the sample from 81 to 21 vol.%.

Acknowledgements

The authors thank gratefully the Foundation for Science and Technology of Portugal for its financial support.

References

1. Jeng, Y. L. and Lavernia, E. J., Review processing of molybdenum disilicide. *J. Mater. Sci.*, 1994, **29**, 2557–2571.
2. Costil, V., *Elaboration et Caractérisation du Disiliciure de Molybdène Renforcé par des Plaquettes d'Alumine*. Thesis, INSA Lyon, N°97-ISAL 0104, 1997.
3. Zhang, S. and Munir, Z. A., Synthesis of molybdenum silicides by the self-propagating combustion method. *J. Mater. Sci.*, 1991, **26**, 3685–3688.
4. Kharatyan, S. L. and Sarkisyan, A. R., SHS densification of complex silicides: promising materials for the electronics and electrotechnical industries. *Int. J. of SHS*, 1993, **2**(4), 323–332.
5. Tuffé, S. C., Plucknett, K. P. and Wilkinson, D. S., Processing and mechanical properties of alumina platelet reinforced molybdenum disilicide laminates. *Ceram. Eng. Sci. Proc.*, 1993, **14**(9–10), 1199–1208.
6. Maxwell, W. A. and Smith, R. W., Thermal shock resistance and high-temperature strengh of a molybdenum disilicide–aluminum oxide ceramic. NACA Report RM E53F26, October 1953.
7. Shaw, L. and Abbaschian, R., Chemical states of the molybdenum disilicide ($MoSi_2$) surface. *J. Mater. Sci., 30*, 5272–5280.
8. Berztiss, D. A., Cerchiara, R. R., Gulbransen, E. A., Pettit, F. S. and Meier, G. H., Oxidation of $MoSi_2$ and comparison with other silicide materials. *Mater. Sci. Eng.*, 1992, **A155**, 165–181.
9. Wirkus, C. D. and Wilder, D. R., High-temperature oxidation of molybdenum disilicide. *J. Am. Ceram. Soc.*, 1966, **49**(4), 173–176.
10. Lin, W. Y., Hsu, L.-Y. and Speyer, R. F., Stability of molybdenum disilicide in combustion gas environments. *J. Am. Ceram. Soc.*, 1994, **77**(5), 1162–1168.
11. Lin, W. Y., Hsu, L.-Y., Berta, Y. and Speyer, R. F., Combustion gas corrosion resistance of heat exchange materials and refractories for glass furnaces at high temperature: part I, silicon carbide and molybdenum silicide. *Am. Ceram. Soc. Bull.*, 1994, **73**(2), 72–78.
12. Sadananda, K., Feng, C. R., Jones, H. N. and Petrovic, J. J., Creep of molybdenum disilicide composites. *Mater. Sci. Eng.*, 1992, **A155**, 227–239.
13. Vasudévan, A. K. and Petrovic, J. J., A comparative overview of molybdenum disilicide composites. *Mat. Sci. Eng.*, 1992, **A155**, 1–17.
14. Evans, A. G. and Fu, Y., Mechanical behavior of alumina: a model anisotropic brittle solid, in advances. In *Advances in Ceramics*, Vol. 10, *Structure and Properties of MgO and Al_2O_3*, ed. W. D. Kingery. 1984, pp. 697–719.
15. Clarke, D. R., High-temperature deformation of a polycristalline alumina containing an intergranular glass phase. *J. Mater. Sci.*, 1985, **20**, 1321–1332.
16. Huffadine, J. B., The fabrication and properties of molybdenum disilicide and molybdenum-disilicide-alumina. In *Special Ceramics*, ed. P. Popper. Academic Press, New York, 1960, pp. 220–236.

17. Dumont, A.-L., *Composites $MoSi_2/Al_2O_3$: Élaboration à Partir de Réactions Auto-Entretenues (SHS) et Caractérisations*. Thesis, Université de Limoges, no. 12-1999, 1999.
18. Dumont, A.-L., Smith, D. S., Gault, C. and Bonnet, J.-P., Preparation of $MoSi_2/Al_2O_3$ type composites by SHS. *Ann. Chim. Sci. Mater*, 1998, **23**, 11–18.
19. Dumont, A.-L., Smith, D. S., Gault, C. and Bonnet, J-P., Preparation and densification of $MoSi_2/Al_2O_3$-based composites using self-propagating high-temperature synthesis. *Int. J. SHS*, 1998, **7**(2), 269–279.
20. Dumont, A.-L., Gault, C. and Bonnet, J.-P., Mechanical properties of $MoSi_2$–Al_2O_3 composites processed by SHS. *Proc. of 12th Intern. Conf. Comp. Mater. ICCM 12*, 5–9 July, 1999, Paris.
21. Bonnet, J.-P., Désiles, S., Dumont, A. L., Chartier, T., Smith, D. S. and Gault, C., Multilayer $MoSi_2$–Al_2O_3 component prepared by combining tape-casting and SHS process. *Int. J. SHS* 3(8), 1999.
22. Thermodynamic values concerning the species used in this work, from Thermodata data bank.
23. Chartier, T., *Tape Casting, Encyclopaedia of Advanced Materials*. ed. D. Bloor, R. J. Brook, M. C. Flemings and S. Mahajan, Pergamon Press, Oxford, 1994, pp. 2763–2767.